Current Biology, Vol. 12, 369–377, March 5, 2002, ©2002 Elsevier Science Ltd. All rights reserved. PII S0960-9822(02)00716-9

How Myxobacteria Glide

Charles Wolgemuth,[1,5] Egbert Hoiczyk,[2,5] Dale Kaiser,[3] and George Oster[1,4]
[1]Department of Molecular and Cellular Biology and ESPM
University of California, Berkeley
Berkeley, California 94720-3112
[2]Howard Hughes Medical Institute
Laboratory of Cell Biology
Rockefeller University
New York, New York 10021-6399
[3]Department of Biochemistry
Stanford University
Stanford, California 94305

Summary

Background: Many microorganisms, including myxobacteria, cyanobacteria, and flexibacteria, move by gliding. Although gliding always describes a slow surface-associated translocation in the direction of the cell's long axis, it can result from two very different propulsion mechanisms: social (S) motility and adventurous (A) motility. The force for S motility is generated by retraction of type 4 pili. A motility may be associated with the extrusion of slime, but evidence has been lacking, and how force might be generated has remained an enigma. Recently, nozzle-like structures were discovered in cyanobacteria from which slime emanated at the same rate at which the bacteria moved. This strongly implicates slime extrusion as a propulsion mechanism for gliding.

Results: Here we show that similar but smaller nozzle-like structures are found in *Myxococcus xanthus* and that they are clustered at both cell poles, where one might expect propulsive organelles. Furthermore, light and electron microscopical observations show that slime is secreted in ribbons from the ends of cells. To test whether the slime propulsion hypothesis is physically reasonable, we construct a mathematical model of the slime nozzle to see if it can generate a force sufficient to propel *M. xanthus* at the observed velocities. The model assumes that the hydration of slime, a cationic polyelectrolyte, is the force-generating mechanism.

Conclusions: The discovery of nozzle-like organelles in various gliding bacteria suggests their role in prokaryotic gliding. Our calculations and our observations of slime trails demonstrate that slime extrusion from such nozzles can account for most of the observed properties of A motile gliding.

[4]Correspondence: goster@nature.berkeley.edu
[5]These authors contributed equally to this work.

Introduction

Certain bacteria move many cell lengths over surfaces in the direction of their long axis, unaided by flagella, in a process called "gliding" ([1, 2] and references therein). Genetic and cell behavioral studies have shown that there are two distinct mechanisms for gliding motion: adventurous (A) motility and social (S) motility in *M. xanthus* [3]. In many cases, only one of the two propulsion mechanisms is present. Myxobacteria possess both propulsion systems and use them synergistically. While A^-S^- strains are nonmotile, never moving more than 1/4 a cell length [1], both A^+S^- and A^-S^+ strains are motile. However their swarm patterns and swarming rates differ from A^+S^+ [3–5].

Recent studies have shed light on the cellular machinery that drives each of these modes of locomotion. S motility is driven by type 4 pili which appear to extend, attach to nearby cells, and then retract, pulling the cells together [6–10]. The pilT protein has been implicated as the force-generating motor for pilus retraction [6]. The mechanism underlying A motility is less certain, but recent ultrastructural studies have revealed a new organelle in gliding cyanobacteria that offers a candidate for the A motility motor [11, 12]. Because gliding *Myxobacteria* leave trails of slime, release of slime was suggested to propel gliding *Myxobacteria* more than 75 years ago [13, 14]. Evidence that links slime secretion to A motility is found in the phenomena of elasticotaxis: the A motility-dependent movement of cells oriented along lines of stress in agar [15]. Five different A^- mutants but none of the S^- mutants tested were found deficient in elasticotaxis [16]. Elasticotaxis is thought to arise from the tendency of the polyelectrolyte chains of extruding slime to align with polymer chains in the agar substratum on which the cells are gliding. When substrate chains have a preferred orientation, as in stressed agar, the bacteria will glide in that direction. The propensity of myxobacteria to glide on slime trails laid down by other cells could arise similarly [17]. However, direct evidence for such a motor was not forthcoming for any glider, until Hoiczyk and Baumeister found a nozzle-like organelle in the filamentous cyanobacteria, whose secretion rate exactly matched the filaments' locomotion velocity [11, 12]. Here we present evidence that a similar organelle is present in *M. xanthus*. Moreover, in both cyanobacteria and myxobacteria, the nozzles are located appropriately for propulsion. Comparisons between slime secretion in the trails of A^+S^+, A^+S^-, and A^-S^+ mutant strains reinforce the argument that slime secretion is the A motility motor.

To demonstrate that slime propulsion can indeed work as the gliding motor, we present a model for how slime secretion can propel adventurous motility based on the nozzle structure. We propose that the propulsive force is generated by the hydration-driven swelling of the polyelectrolyte slime in the nozzle. We compute the force generated by such a device and show that the number of nozzles found in cyanobacteria and myxo-

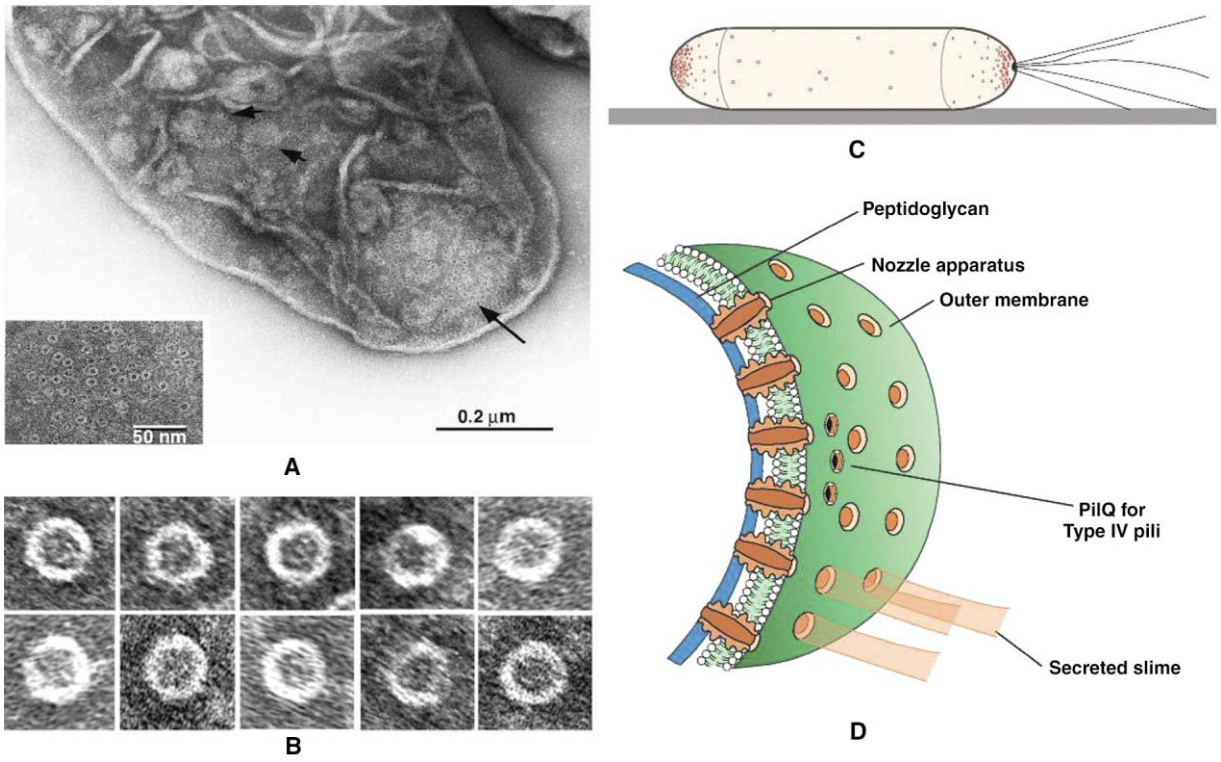

Figure 1. Slime Nozzles

(A) Electron micrograph of a negatively stained isolated cell envelope of *M. xanthus* DK1622, an A^+S^+ strain, showing one of the cell poles. The nozzles are visible as ring-shaped structures which are clustered at the poles (long arrow). Along the rest of the cell surface, the density of nozzles is much smaller (short arrows). The inset shows a higher magnification of the nozzle array in the region indicated by the long arrow. Scale bars are 0.2 μm and 50 nm (inset).

(B) A gallery of electron micrographs of negatively stained isolated nozzles from *M. xanthus* DK1622. In these top views, each cylindrically symmetric nozzle has an outer diameter of ~14 nm, with a central hole of ~6 nm. The diameter is similar to the corresponding structures found in cyanobacteria, suggesting that the remainder of the nozzle may be of similar size.

(C) Schematic illustration of the arrangement and location of the different cellular structures involved in gliding motility in *M. xanthus*. Nozzles are clustered at the two cell poles, pili at one pole. S motility is generated by the pili, which extend, attach to nearby cells, and then retract, pulling the cells together. We propose that A motility is driven by the secretion of mucilage from the nozzles (indicated as small circles). As the mucilage adheres to the substrate, further secretion drives the cell in the opposite direction. The observed reversals of movement would be caused by alternation of the active polar nozzle cluster.

(D) Cartoon illustrating the proposed layout of the nozzles in the polar region shown in (A). The nozzle cross-sections shown are drawn with the same geometry as those found in cyanobacteria, c.f. [12].

bacteria are sufficient to propel the cell at the observed velocities. The model also explains a variety of other observations on adventurous gliding motility and suggests experiments that can help establish this as the A motility motor.

Results

Myxococcus and Cyanobacteria Possess Similar Nozzle Structures

A characteristic feature of the cell envelopes of gliding cyanobacteria is the presence of nozzle-like organelles from which the bacteria secrete mucilage while moving [12]. As *Myxococcus* cells also deposit slime trails during locomotion, we searched for the presence of similar organelles in the myxobacterial cell wall. Using negatively stained whole cells and isolated cell envelopes, ring-like structures were detected which were strikingly similar to the nozzles, or junctional pore complexes, of cyanobacteria. Each of these ring-like structures in *Myxococcus* consisted of an opaque core of about 6.5 nm surrounded by a less electron dense peripheral zone 12–14 nm in diameter. Aside from their slightly smaller diameter, these structures were virtually identical to their cyanobacterial counterparts, an observation which is all the more remarkable given that these two bacterial groups are not closely related phylogenetically [18]. Closer inspection of the *Myxococcus* cells showed that the nozzles have a distinct spatial distribution: up to 250 nozzles were clustered at each of the two opposite cell poles, while in-between only a few scattered pores were found (see Figure 1). Pores are also formed by the ring-forming outer membrane protein PilQ, a component of the type 4 pili S motility apparatus [19]. In order to rule out that the pores were formed by PilQ, we also studied Δ*pilQ*, Δ*pilH*, Δ*cglB*, and Δ*mglA* strains. All these mutants, including a *pilQ* deletion mutant, still possessed the nozzles, confirming that this structure was not part of the S motility machinery. Interestingly,

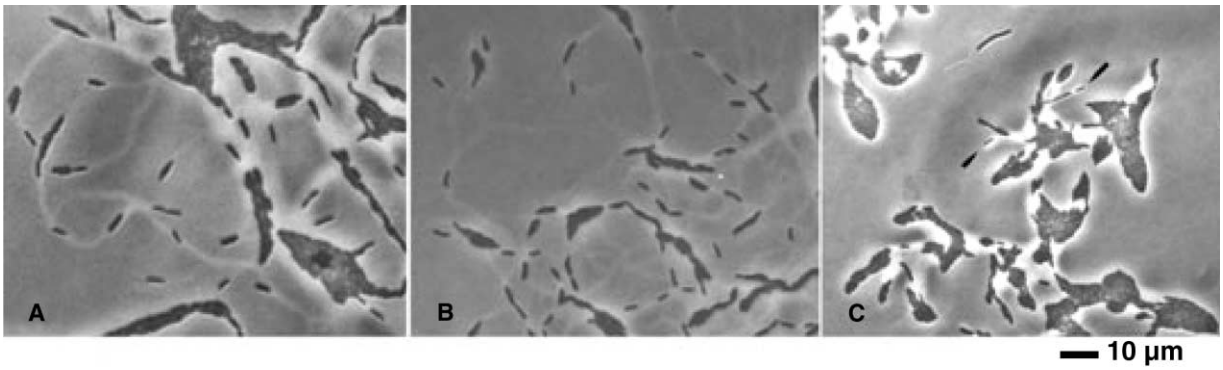

Figure 2. Slime Trails

Deposition of slime by *M. xanthus* as it glides on agar. (A) A^+S^+ strain DK1622. (B) A^+S^- strain DK10410. (C) A^-S^+ strain ASX1. Photographs of the swarming edge were taken after 1 day.

the nozzles were also present in cells carrying a mutation of the *mglA* gene, the only known gene required for both A and S motility [4, 20]. Overall no difference in the number or arrangement of the nozzles in these four mutants were detected compared with the *Myxococcus* A^+S^+ cells.

In order to further compare the molecular architecture of the myxobacterial and cyanobacterial nozzles, we tried to isolate the nozzles from *Myxococcus*. Isolated cell envelopes were solubilized and fractionated as described in Experimental Procedures. Using detergent treatment, fractions containing isolated nozzles were obtained. All of these nozzle preparations yielded exclusively top-view orientations of the particle (see Figure 1). Measurement of the nozzles in this projection showed an outer diameter of ~14 nm and an inner hole of ~6.5 nm. Individual nozzles had a cylindrical symmetry and were virtually identical to the nozzles found in cyanobacteria. So far, however, we have not determined whether the nozzles in *Myxococcus* are also part of a larger organelle-like structure as in their cyanobacterial counterparts [12].

Observations of Slime Trails

Gliding myxobacteria leave trails of slime behind them, and other cells prefer to move on such trails [21, 22]. If A motility is driven by the secretion of slime which is left behind as a trail, while S motility is driven by the retraction of pili, then the trails left by the two might be different. Figure 2 shows phase contrast micrographs of cells at the edge of their swarms with their associated slime trails. Slime trails are visible due to the difference in refractive index between the slime gel and the agar gel. The trails of an A^+S^+ strain (Figure 2A, DK1622) and of an A^+S^- strain (Figure 2B, DK10410) that is unable to produce pili because it is deleted for *pilA* are similar. An A^-S^+ strain (ASX1) that is deleted for *cglB*, a cell surface protein [23], is shown in Figure 2C. Because A^-S^+ swarms normally produce only wide, many cell layered peninsulas that cover their trails, a young and still thin swarm edge was very gently respread after a day to obtain a single cell layer of rafts and single cells. The respread plates were then incubated 2 days to allow the cells to move using S motility and to expose the slime trails. As shown in Figures 2A and 2B, the A^+S^+ cells and the A^+S^- cells leave trails as wide as the cell body, or bodies, that apparently produced them. Typically, trails extend from both ends of cells because cells reverse direction every few minutes. Comparison of Figure 2A (S^+) with Figure 2B (S^-) shows no effect of the presence or absence of S motility in the trails. Thus, the type 4 pili are not needed to form or to follow a slime trail. The A^-S^+ cells do not leave trails like the A^+S^+ or the A^+S^- strains. Instead of a trail, there is a phase bright area around each isolated cell. Several examples are shown in Figure 2C. Because isolated A^-S^+ cells do not move unless they are within a pilus length of another cell [5], presumably, these cells were resting in place. The phase bright area is distributed uniformly around these cells. Phase bright areas are also evident around and behind the rafts, which likely had moved forward by their pilus-mediated S motility. These phase bright areas are wider (per cell) than the trails of A motile or wild-type cells (Figures 2A and 2B). The phase bright areas, having about the same refractive index as trails of groups of A^+S^+ cells in Figure 2A, appear to be puddles of slime that had been secreted uniformly around the cells instead of predominantly from their poles.

The Nozzles of *M. xanthus* Are Involved in Slime Secretion

As indicated by the different slime secretion pattern of various *M. xanthus* strains, the secretion of mucilage seems to play an important role in gliding motility. These observations, together with the discovery of clusters of nozzles at the cell poles, prompted us to test whether the nozzles are the sites of mucilage secretion as in cyanobacteria. [12]. In order to study the slime secretion process in greater detail, we first examined the secretion of *M. xanthus* wild-type cells using a fluorescent light microscope. Acridine orange was used to visualize the secreted and deposited slime trails left behind by the moving cells. Each individual cell thereby leaves a trail behind which originates from its rear cell pole (Figure 3A). If slime trails were used repeatedly by gliding cells, increasingly more material was deposited and the trails become more strongly stained. Taken alone, this observation, however, does not prove whether the nozzles

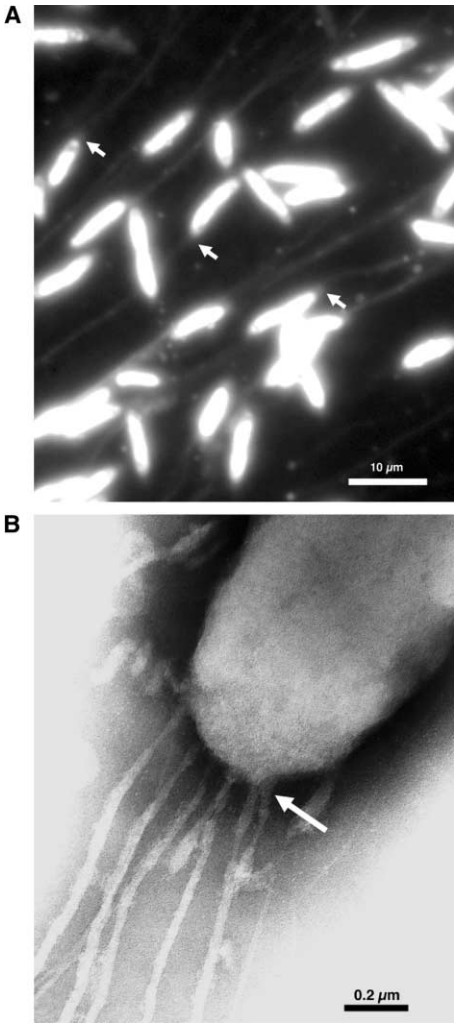

Figure 3. Examination of the Slime Secretion Process in Wild-Type *M. xanthus* Cells

(A) Fluorescent light micrograph of gliding *M. xanthus* cells (A^+S^+ Strain DK1622). During locomotion, the cells leave slime trails behind, which can be stained by Acridine orange. Note that the slime trails originate at the rear poles of the individual cells (small arrows). Photograph taken after 1 hr at 2000×.

(B) Electron micrograph of the cell pole of a gliding *M. xanthus* cell. At higher magnification, it can be seen that the slime trails are composed of several slime bands, which are secreted from the sites at the cell pole, where the nozzles are located (large arrow).

are the actual sites of slime secretion, given the low resolution of the light microscope. In order to examine the role of the nozzles in slime secretion in greater detail, *M. xanthus* cells were allowed to glide over electron microscopic grids and then negatively stained. Examination of such cells at high magnification showed that the deposited slime trails are made up of a variable number of slime bands which originate at the cell poles where the clusters of nozzles are located (Figure 3B). Consistent with the observation that some nozzles are scattered over the entire surface of the bacterial cell, it was also found that the cells could secrete small amounts of slime at sites other than the cell pole (data not shown). Whether this additional slime plays a role in motility or is involved in the attachment and lubrication of the cell's surface is not clear. Although we cannot completely rule out that negative staining might alter the appearance of the slime, the origination of the bands at the cell poles strongly suggests that the nozzles of *M. xanthus* are the sites of slime secretion during motility. Finally, fluorescence and electron microscopy of nonpiliated A^+S^- mutants showed that these cells secreted slime trails, which are identical to the ones deposited by wild-type cells.

A Model for Nozzle Function

Based on high-resolution pictures of the nozzle structure in cyanobacteria, we propose a model for how slime secretion can drive A motility. Slime is imported into the proximal end of the nozzle, near the inner membrane. This slime is hydrated by water that flows into the nozzle from outside the cell, causing the slime to swell. This expansion drives the slime out of the nozzle, producing a propulsive thrust. To evaluate whether the swelling of the slime gel would be sufficient to account for the propulsion of the bacterium, we compute the force exerted by the swelling of the slime at the nozzle exit. The model consists of two parts: the nozzle assembly and the slime gel. We will describe each component qualitatively; the mathematical details are presented in the Supplementary Material available with this article online.

The Nozzle Assembly

The shape and size of the nozzle is constructed from the electron micrographs of Hoiczyk and Baumeister [12]. Figure 4A shows the nozzle geometry. There are certain important features that are not discernable from the micrographs, and so we have investigated various designs. For example, the averaged micrographs do not contain sufficient detail to ascertain if the midbody of the nozzle is perfectly cylindrical. There is the suggestion that there is a central bulge that, if present, confers certain mechanical advantages, and so we investigated both designs. Also, it is not possible to deduce what portions, if any, of the nozzle are permeable to water. Since the swelling of the gel provides the propulsive force, the pattern of fluid flow within the nozzle is important. Therefore, we investigated several plausible permeability patterns to ascertain the best design. Mechanically, we shall assume that the nozzle walls are perfectly rigid. This is clearly an approximation, but the micrographs give the impression that the nozzle is circumferentially reinforced (like barrel hoops).

The Slime Gel

The chemical composition of the slime has not been completely characterized. However, it is clear that it constitutes a polyelectrolyte gel. Therefore, we can model it after other gels, such as snail slime, which are likely to have similar properties. It will turn out that our conclusions are not very sensitive to the details of the slime chemistry. The attribute of the slime gel that allows it to generate a propulsive force is its hydration power, a property characteristic of polyelectrolyte gels (Figure 5). Several forces contribute to the osmotic swelling pressure, Π, of a polyelectrolyte gel [24]:

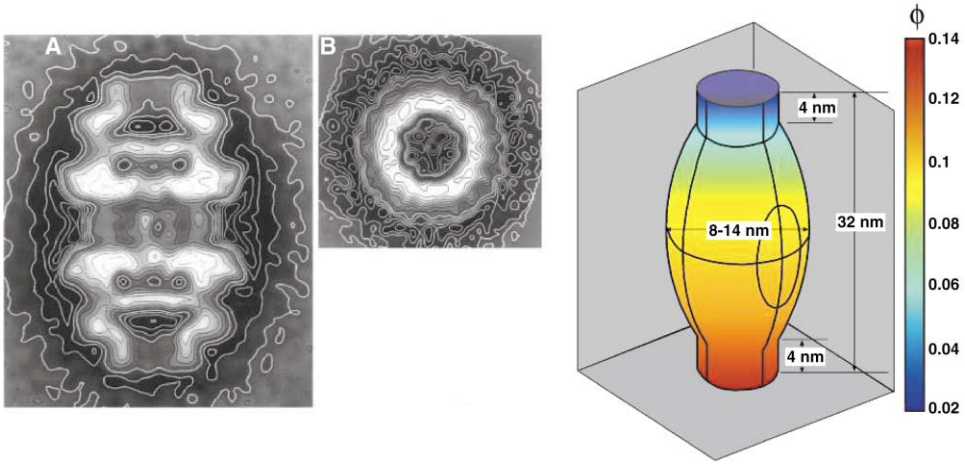

Figure 4. Geometry of the Slime Nozzle

(Left panel) Longitudinal and cross-sectional view of the juctional pore complex in *P. uncinatum*, from [12]. (Right panel) Geometry of the finite element model of the junctional pore complex. The width of the central bulge is variable.

$$\Pi = \Pi_{Entropic} + \Pi_{Ion} + \Pi_{Elastic} + \Pi_{Interaction} \quad (1)$$

The terms in equation (1) are

- $\Pi_{Entropic}$: The gel fibers tend to diffuse outward into the surrounding fluid, just as if they were disconnected.
- Π_{Ion}: A polyelectrolyte gel contains diffusible counterions to the negative charges fixed on the gel fibers. The counterions create an "ion gas pressure" that tends to swell the gel. The ions are prevented from escaping the gel by the electrical double layer surrounding the gel. This electrical boundary develops a Donnan potential that acts as a membrane—perfectly permeable to water but impermeable to the counterions.
- $\Pi_{Elastic}$: Since the gel fibers are crosslinked, their elasticity tends to resist its tendency to expand outwards.

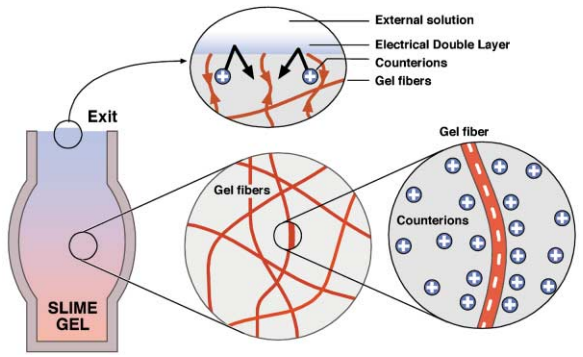

Figure 5. The Slime Comprises a Polyelectrolyte Gel Consisting of a Crosslinked and Entangled Network of Fibers

Along each fiber is a distribution of charged sites that attract a counterion cloud. The counterions can be viewed as a gas that tends to inflate the gel. Macroscopically, the gel is electrically neutral, but at the gel surface a Donnan potential is generated by the mobile counterions. This electrical field acts as a perfect semipermeable membrane, allowing water to pass but preventing the ions from leaving the gel. The nozzle is assumed to hydrate only through the nozzle exit, so that a hydration gradient exists along the nozzle.

- $\Pi_{Interaction}$: Several effects conspire to set up an attraction between the gel fibers that resists the swelling effects of the first two factors.

The Supplementary Material describes these effects quantitatively and in more detail. The gel osmotic pressure, Π_{Total}, tends to swell the gel. Since the gel is an elastic body, in addition to swelling, it develops shear deformations that reduce the swelling force somewhat. However, since the gel is confined to the nozzle, swelling is directed toward the nozzle opening. The pattern of swelling depends on the pathways for water entering the gel. We have investigated two possibilities: (1) the nozzle walls are impermeable, so that water enters the nozzle only through the distal open end; and (2) the walls are permeable, so that hydration water can enter the sides as well. The goal of the model is to compute the force generated at the nozzle opening (i.e., the swelling pressure times the cross-sectional area at the opening).

Finally, the model does not address the issue of how the gel is introduced into the nozzle. The mechanism is not known, and so we simply assume that the proximal end of the nozzle is held at an initial gel volume fraction, ϕ_{init} = gel volume/(gel volume + water volume). We can speculate on several possible mechanisms. For example, gel monomers might be transported through the proximal walls and polymerized inside the nozzle. Alternatively, the gel could be introduced in a deswelled state by the presence of divalent cations. In eukaryotes, secretory vesicles containing mucin are kept in a deswelled state by the presence of divalent cations, especially Ca^{2+} [25]. Ca^{2+} is a powerful gel deswellant, while univalent cations such as Na^{+} are not. Thus, near the nozzle exit, divalent ions would diffuse out down their concentration gradient, replaced by inward diffusing Na^{+} and K^{+} in stoichiometric amounts so as to maintain electrical neutrality. In this scenario, the bulk of the swelling would take place near the nozzle exit. *M. xanthus* requires external calcium for A motility [28, 29]. This makes sense in the context of our calculations, since the thrust is generated by a modest expansion in

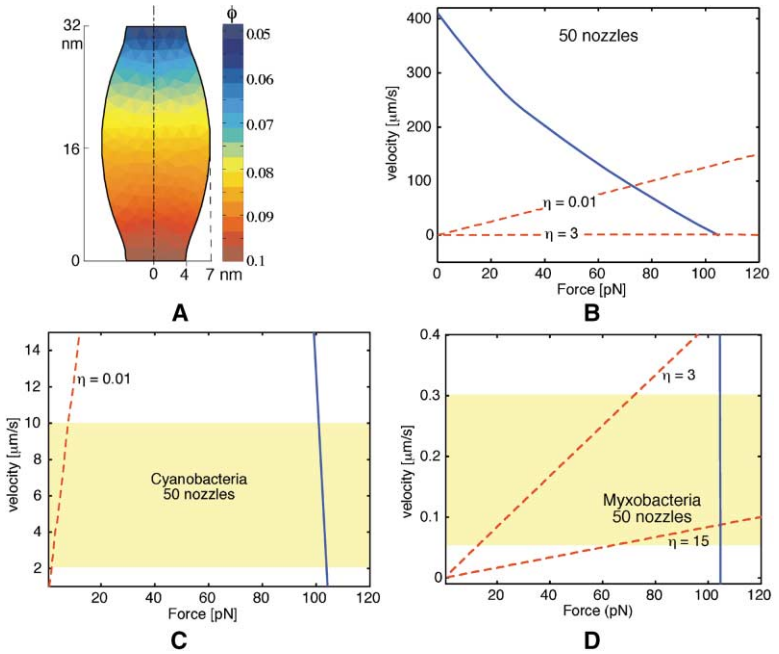

Figure 6. Results of the Slime Nozzle Model

(A) Cross-section of the finite element model of a nozzle showing the gel fraction, ϕ.

(B) Load-velocity curve for 50 slime nozzles.

(C and D) Load-velocity curves for cyanobacteria (C) and *M. xanthus* (D), demonstrating that only 50 working nozzles suffice to drive both species at their observed speeds. Shaded regions denote the observed speed range for either cyanobacteria or myxobacteria, respectively; dashed lines plot viscous drag force acting on a cylindrical cell immersed in media of viscosities 0.1, 3, and 15 Poise; and solid lines plot the propulsive thrust from the nozzles.

volume fraction from ~5% to ~2%. In the absence of external calcium, the gel would expand too much upon extrusion, so that its compressive modulus would likely be too small to support much thrust. However, in the simulations shown below, an ion exchange process at the nozzle exit is not computed explicitly.

Results of the Nozzle Model

The question the model addresses is whether the osmotic expansion of the slime from the nozzle generates sufficient force to propel the bacterium at the observed speed. Figure 6A shows a cross-section of the nozzle and the proximal to distal profile of the gel volume fraction. In our simulations, we introduce the gel at a volume fraction of 5%–6%, during its exit from the nozzle it swells to 2%–3%. We show that this model provides ample force to drive the bacterium.

The drag force that must be overcome by the propulsive thrust can be estimated by assuming that the bacterium is a cylindrical filament in a viscous fluid of viscosity, η. The drag force, $F_{Drag} = \zeta \times v$, where v is the bacterial velocity and ζ its drag coefficient. For a cylinder of length L and radius r moving in a medium of viscosity η, ζ, is computed from $\zeta = (2\pi\eta L)/[\cosh^{-1}((r + \delta)/r)]$, where δ is the thickness of the slime, i.e., the distance from the cell surface to the surface of the substrate [26]. Figure 6B shows the complete force-velocity curve computed at the exit for 50 nozzles. However, the operating region for both cyanobacteria and myxobacteria occupy only a small region of this curve, since they are operating very close to their stall force.

From the micrographs in Hoiczyk and Baumeister [12], we estimate there are about 500 nozzles around the circumference of each end of each cell in a cyanobacterial filament. Taking into account that only slime from one sector of the circumference interacts with the substratum, we estimate a lower bound of 50 nozzles are working to produce thrust. *M. xanthus* has fewer nozzles, but from Figure 1 we estimate a similar lower bound for the number of working nozzles whose slime first contacts the substratum. Using 50 nozzles, Figures 6C and 6D show a closeup of the regions wherein cyanobacteria and myxobacteria operate, respectively. We see that, over a wide range of slime viscosities, the thrust from 50 slime nozzles would be sufficient to account for the gliding velocities of both species. We emphasize that this is a conservative lower bound for the number of working nozzles; in the Supplementary Material, we show that this conclusion is rather insensitive to the particular parameter values we have selected. Therefore, we conclude that the thrust generated by a modest hydration of the slime extruding from the nozzles of both species provides more than enough force to account for the observed gliding speeds.

The slime propulsion mechanism is consistent with the phenomenon of slime trail following and elasticotaxis discussed above [15, 16]. If the exuded slime adhere more strongly to other slime than to the agar substratum, then a moving bacterium encountering a transverse slime trail will be pivoted into alignment with it by the rear end thrust of the nozzles, where after it will continue to move along the trail where its adhesion is strongest. In elasticotaxis, the slime must attach to the solid component of the agar. Therefore, alignment of the slime filaments with those of the strain-aligned substratum filaments provide more adhesive sites for developing traction. This favors propulsion along strain lines, analogous to the alignment of fibroblasts along traction-generated strains in extracellular matrix [27].

Finally, we note that the issue of force generation is distinct from the energy required for propulsion. Knowing the drag force on the cell and the velocity of the cell, one can compute the power required to propel the cell at the observed velocity. However, this does not address the question of how the propulsive force is

generated. Energy calculations only tell what is possible, saying nothing of the mechanism. The model proposes that the propulsive power comes from hydration of the gel, which is dependent on fluid flow and polymer concentration. This power does not directly depend on the metabolism of the cell. Polymer production does, however, and is surely a metabolic cost to the cell. If the propulsive power were greater than the production cost, then the cell would get more energy out of the system than it put in and would violate the first law of thermodynamics. In the Supplementary Material, we estimate the metabolic cost of slime production; of course, it is more than the energy consumption due to gliding.

Discussion

In this study, we have shown that *M. xanthus* possess nozzle-like structures, which are structurally similar to the nozzle-like organelle found in gliding cyanobacteria. Although the myxobacterial nozzles have a slightly smaller diameter, the overall similarity of these two structures is quite striking and all the more remarkable given that these two bacteria groups are not closely related [18]. Interestingly, some descriptions in the literature suggest that even more gliding prokaryotes possess such nozzle-like structures. The rotary assemblies in *Cytophaga johnsonae* and *Flexibacter columnaris* [30] resemble nozzles, in which case they would support a widespread distribution of such structures among gliding bacteria. In addition, in many of these bacteria, including the cyanobacteria, *C. johnsonae*, and *F. columnaris*, the nozzles are only present in motile strains but absent from nonmotile strains. Altogether, these observations suggest that the nozzles represent a highly conserved type of organelle involved in gliding motility in these species.

Although the proteins associated with slime secretion have yet to be identified, their similar appearance in phylogenetically distant organisms suggests a common function. We have presented five independent lines of evidence that suggest that the nozzles are the molecular motor of gliding motility. First, studies in cyanobacteria indicate that the nozzles are involved in the secretion of slime and that the rate of slime extrusion in these bacteria matches the observed speed of gliding. Second, in *M. xanthus* the nozzles are clustered predominantly at the poles appropriately located for propulsion. In cyanobacteria, each cell within the multicellular filaments possesses two alternate sets of pores pointing in opposite directions. Third, the pattern of slime secretion in A^+S^+, A^-S^+, and A^+S^- strains of *M. xanthus* indicates that slime secretion is associated with A motility. Fourth, electron microscopic studies of *M. xanthus* suggest that the nozzles are indeed the sites of slime secretion, as they are in cyanobacteria. And fifth, a quantitative analysis of the slime nozzle mechanism demonstrates that it can generate sufficient force to drive cell motions at the observed velocities.

The arrangements of the nozzles not only offer an explanation for motility in these species but also for the observed frequent reversals of movement. These reversals might result from an alternation of the sets of pores used. If only those pores at one cell pole secrete slime, a directed movement forward or backward will result.

Several other models for A motility in *M. xanthus* have been proposed. One by Dworkin and Keller [31, 32] proposes that bacteria secrete a surfactant from unidentified organelles on the ventral surface. The surfactant creates a gradient in the interfacial tension gradient in the substratum that pulls the bacterium forward. Spormann [1] and Berg and Lapidus [33] have proposed models with numerous force generators distributed over the cell surface. Lunsdorf found circularly twisted protein bands in electron micrographs and attributed to them a role in A motility [34–36]. Our data do not disprove these models, but we believe the evidence for them is insufficient to account for A motility. Nor are these models exclusive of the model presented here: we note that the nozzles are distributed over the cell surface and that the slime secreted by them likely has surfactant properties. Based on our results that the pores are present at high density at both cell ends, we propose that slime is propelled from only one end at a time but can be switched to the other end when A motility reverses direction. Pores are also present at lower density over the entire surface and secrete some slime constitutively over the whole cell; this might serve as a lubricant and as an adhesive that attaches a cell to the surface of its substratum.

Although our calculation based on the pore size supports the slime propulsion mechanism for A motility, we cannot yet specify the proteins involved. The challenge remains to correlate slime propulsion with particular defects in A motility. The slime propulsion mechanism predicts A^- mutants that would display obvious defects in the nozzle apparatus, whether in structure, number, or distribution. Other A^- mutants might have normal pores but possess defects in the biochemical pathway that supplies slime to the nozzle or in the properties of the slime itself. Despite the number of possibilities, there is now a prima facie case for the slime propulsion model, since it explains—or is consistent with—the phenomena associated with A motility and now rests on clear anatomical and solid biophysical foundations.

Conclusions

Here, we have shown that phylogenetically unrelated gliding bacteria, such as *M. xanthus* and cyanobacteria, possess similar nozzle-like organelles. As these bacteria secrete mucilage during locomotion, which originates from cell ends where the nozzles are located, it is plausible to assume that these structures function as A motility motors. This assumption is supported by the observation that the nozzles are (1) widespread among gliding bacteria, (2) involved in slime secretion, (3) appropriately located for propulsion, and (4) can generate sufficient force to propel the cells at the observed speeds. Our calculations suggest furthermore that secretion-based propulsion is a robust process that depends only on the polyelectrolyte properties of the slime, not its particular chemical composition or the surface properties of the substrate, other than that slime adheres to it.

Experimental Procedures

Bacterial Strains, Media, and Cultivation

The *M. xanthus* strains used in this study were (1) DK 1622 (phenotype A^+S^+); (2) DK 8615, Δ*pilQ* and DK 11133, Δ*pilH* (both with an A^+S^- phenotype); (3) DK 10410, Δ*pilA* and ASX1, Δ*cglB* (Rodriguez); and (4) DK 6204, Δ*mglAB*, which carries a knockout in two genes necessary for both A and S motility (phenotype A^-S^-). All these deletions are nonpolar. A more detailed description of the strains has been given elsewhere [3, 4, 23, 37]. *M. xanthus* strains were cultivated at room temperature for cell envelope preparation and at 32°C for slime trail studies in 1/2CTT broth (0.5% bacto casitone, 10 mM Tris-HCl [pH 8.0], 8 mM $MgSO_4$, 1 mM KPO_4 [pH 7.6]) or on 1/2CTT agar (1/2CTT broth plus 1.5% agar).

Cell Envelope Preparation

Cells of the various *M. xanthus* strains were either washed off the CTT agar plates or grown in CTT broth and harvested by centrifugation (15 min at 10,000 × *g*). The cells were then suspended either in Tris-buffer (20 mM Tris-HCl [pH 7.5]) or in distilled water containing 10 mM $MgCl_2$, 1 mM phenylmethylsulfonyl fluoride, and 50 mg/ml DNase II and broken by two passages through a french press (Aminco Instruments) at a pressure of 600 psi. Unbroken cells were removed (10 min, 10,000 × *g*), and the cell envelopes were sedimented at 40,000 × *g* for 20 min and washed twice with Tris-buffer.

Isolation of the Myxobacterial Nozzles

Isolated and purified cell envelopes were suspended in Tris-buffer (20 mM [pH 7.5]) containing 2% digitonin and slowly shaken at room temperature for 1 hr. After incubation, unsolubilized envelope fragments were removed by centrifugation (20 min at 40,000 × *g*) and the suspension subjected to ultracentrifugation (1 hr at 100,000 × *g*). Finally, nozzle complexes were sedimented by centrifugation (2 hr at 300,000 × *g*), resuspended in a drop of Tris-buffer, and used for negative staining.

Specimen Preparation and Electron Microscopy

Whole cells and isolated cell envelopes of the different *M. xanthus* strains were applied to glow-discharged carbon-coated grids and negatively stained with 2% (w/v) unbuffered uranyl acetate or 1.5% (w/v) sodium phosphungstate at pH 7.2. In order to screen all cells of a colony spreading on CTT agar, samples were taken at various distances from the fringe of the colony. All specimens were examined with a Philips CM12 electron microscope at an operating voltage of 100kV and a nominal magnification of 45,000×.

Observation of Slime Secretion

A 10 μl droplet containing 5×10^6 exponentially growing *M. xanthus* cells was placed in the center of a 5 cm diameter petri dish. The dish contained 3.5 ml of 1/2CTT 1.5% agar. After the droplet had dried, the plate was sealed and incubated at 32°C for swarming. After the time period indicated, the cover was removed from the dish, and the edge of the swarm was examined with a 16× or 20× phase contrast objective illuminated through the thin layer of agar. Photographs were taken with Kodak Tmax 100 black and white film. In addition, droplets of 1/2CTT broth containing motile *M. xanthus* cells were placed on glass slides. The slides were kept without coverslips in a wet chamber to prevent drying. After incubation of the samples at room temperature for 1–5 hr, the cells and slime trails were stained with 0.1% acridine orange for 2 min and examined with a Zeiss™ fluorescent microscope (filter combination, FT 510 and LP 520). Photos were recorded either with a digital camera (Hamamatsu, Ichinocho, Japan) using the program Openlab™ (Improvision, Lexington, KY) or taken with Kodak Ektachrome™ 400X film. In order to correlate the slime secretion process with the location of the pore complexes at the cell poles, small droplets containing *M. xanthus* cells were placed on carbon-coated gold grids (400 mesh). The grids were incubated in a wet chamber for 15 min to 2 hr, stained with 1.5% sodium or silico phosphungstate at pH 7.4, and viewed in the electron microscope.

Supplementary Material

Supplementary Material including details of how the model of slime hydration was constructed and the parameter values used to compute the force-velocity relationship can be found at http://images.cellpress.com/supmat/supmatin.htm.

Acknowledgments

David Stokes and Mike Lewis are gratefully acknowledged for use of the electron microscope facility at the Skirball Institute of Biomolecular Medicine; and Yvonne Cheng (Stanford University) for continuous, excellent technical help. David Zusman and his lab were always available for valuable discussions. Tom Powers provided a wealth of perceptive criticisms to the manuscript. C.W. and G.O. were supported by National Science Foundation Grant DMS-9972826 and National Institutes of Health Grant GM59875-01A1; E.H. was supported by a HHMI postdoctoral fellowship; D.K. was supported by NIH grant GM23441.

Received: August 28, 2001
Revised: January 11, 2002
Accepted: January 11, 2002
Published: March 5, 2002

References

1. Spormann, A. (1999). Gliding motility in bacteria: insights from studies of *Myxococcus xanthus*. Microbiol. Mol. Biol. Rev. *63*, 621–641.
2. McBride, M. (2000). Bacterial gliding motility: Mechanisms and mysteries. Amer. Soc. Microbiol. News *66*, 203–210.
3. Hodgkin, J., and Kaiser, D. (1979). Genetics of gliding motility in *Myxococcus xanthus* (*myxobacterales*): genes controlling movement of single cells. Molec. Gen. Genet. *171*, 167–176.
4. Hodgkin, J., and Kaiser, D. (1979). Genetics of gliding motility in *Myxococcus xanthus* (*myxobacterales*): two gene systems control movement. Molec. Gen. Genet. *171*, 177–191.
5. Kaiser, D., and Crosby, C. (1983). Cell movement and its coordination in swarms of *Myxococcus xanthus*. Cell Motil. *3*, 227–245.
6. Kaiser, D. (2000). Bacterial motility: How do pili pull? Curr. Biol. *10*, R777–R780.
7. Merz, A., Sheetz, M., and So, M. (2000). Pilus retraction powers bacterial twitching motility. Nature *407*, 98–102.
8. Sun, H., Zusman, D., and Shi, W. (2000). Type IV pilus of *Myxococcus xanthus* is a motility apparatus controlled by the frz chemosensory system. Curr. Biol. *10*, 1143–1146.
9. Wall, D., and Kaiser, D. (1998). Alignment enhances the cell-to-cell transfer of pilus phenotype. Proc. Natl. Acad. Sci. USA *95*, 3054–3058.
10. Skerker, J.M., and Berg, H.C. (2001). Direct observation of extension and retraction of type IV pili. Proc. Natl. Acad. Sci. USA *98*, 6901–6904.
11. Hoiczyk, E. (2000). Gliding motility in cyanobacteria: observations and possible explanations. Arch. Micro. *174*, 11–17.
12. Hoiczyk, E., and Baumeister, W. (1998). The junctional pore complex, a prokaryotic secretion organelle, is the molecular motor underlying gliding motility in cyanobacteria. Curr. Biol. *8*, 1161–1168.
13. Jahn, E. (1924). Beitrage zur botanischen protistologie. I. Die Polyangiden (Leipzig: Gebrèuder Borntraeger).
14. Kuhlwein, H. (1953). Weitere untersuchungen an myxobacterien. Arch. Mikrobiol. *19*, 365–371.
15. Stanier, R. (1942). Elasticotaxis in *Myxobacteria*. J. Bacteriol. *44*, 405–412.
16. Fontes, M., and Kaiser, D. (1999). *Myxococcus* cells respond to elastic forces in their substrate. Proc. Natl. Acad. Sci. USA *96*, 8052–8057.
17. Burchard, R.P. (1984). Gliding motility and taxes. In Myxobacteria, E. Rosenberg, ed. (New York: Springer-Verlag), pp. 139–161.
18. Woese, C.R. (1987). Bacterial evolution. Microbiol. Rev. *51*, 221–271.
19. Wall, D., Kolenbrander, P., and Kaiser, D. (1999). The *Myxococ-*

cus xanthus pilQ (sglA) gene encodes a secretin homolog required for type IV pilus biogenesis, social motility, and development. J. Bacteriol. *181*, 24–33.
20. Stephens, K., Hartzell, P., and Kaiser, D. (1989). Gliding motility in *Myxococcus xanthus*: mgl locus, RNA, and predicted protein products. J. Bacteriol. *171*, 819–830.
21. Kuhlwein, H., and Reichenbach, H. (1965). Swarming and morphogenesis in *Myxobacteria*. Inst. Wiss. Film, Film C893. Gottingen.
22. Burchard, R. (1982). Trail following by gliding bacteria. J. Bacteriol. *152*, 495–501.
23. Rodriguez, A.M., and Spormann, A.M. (1999). Genetic and molecular analysis of cglB, a gene essential for single-cell gliding in *Myxococcus xanthus*. J. Bacteriol. *181*, 4381–4390.
24. Tanaka, T., Annaka, M., Ilmain, F., Ishii, K., Kofufuta, E., Suzuki, A., and Tokita, M. (1992). Phase transitions of gels. In Mechanics of Swellings, Volume H 64, T.K. Karalis, ed. (Berlin: Springer-Verlag), pp. 683–703.
25. Verdugo, P. (1991). Mucin exocytosis. Am. Rev. Respir. Dis. *144*, 533–537.
26. Hunt, A.J., Gittes, F., and Howard, J. (1994). The force exerted by a single kinesin molecule against a viscous load. Biophys. J. *67*, 766–781.
27. Oster, G., Murray, J., and Harris, A. (1983). Mechanical aspects of mesenchymal morphogenesis. J. Embryol. Exp. Morph. *78*, 83–125.
28. Burchard, R.P. (1974). Studies on gliding motility in *Myxococcus xanthus*. Arch. Microbiol. *99*, 271–280.
29. Womack, B., Gilmore, D., and White, D. (1989). Calcium requirement for gliding motility in myxobacteria. J. Bacteriol. *171*, 6093–6096.
30. Pate, J., and Chang, L. (1979). Evidence that gliding motility in prokaryotic cells is driven by rotary assemblies in the cell envelopes. Curr. Microbiol. *2*, 59–64.
31. Dworkin, M., Keller, K.H., and Weisberg, D. (1983). Experimental observations consistent with a surface tension model of gliding motility of *Myxococcus xanthus*. J. Bacteriol. *155*, 1367–1371.
32. Keller, K.H., Grady, M., and Dworkin, M. (1983). Surface tension gradients: feasible model for gliding motility of *Myxococcus xanthus*. J. Bacteriol. *155*, 1358–1366.
33. Lapidus, I., and Berg, H. (1982). Gliding motility of *cytophaga spec*. strain U67. J. Bacteriol. *151*, 383–398.
34. Lunsdorf, H., and Reichenbach, H. (1989). Ultrastructural details of the apparatus of gliding motility of *Myxococcus fulvus (myxobacterales)*. J. Gen. Microbiol. *135*, 1633–1641.
35. Freese, A., Reichenbach, H., and Lunsdorf, H. (1997). Further characterization and in situ localization of chain-like aggregates of the gliding bacteria *Myxococcus fulvus* and *Myxococcus xanthus*. J. Bacteriol. *179*, 1246–1252.
36. Lunsdorf, H., and Schairer, H.U. (2001). Frozen motion of gliding bacteria outlines inherent features of the motility apparatus. Microbiology *147*, 939–947.
37. Wu, S.S., Wu, J., and Kaiser, D. (1997). The *Myxococcus xanthus* pilT locus is required for social gliding motility although pili are still produced. Mol. Microbiol. *23*, 109–121.